Gene Expression Patterns and Profile Changes Pre- and Post-Erlotinib Treatment in Patients with Metastatic Breast Cancer

Sherry X. Yang,[1] Richard M. Simon,[2] Antoinette R. Tan,[1] Diana Nguyen,[1] and Sandra M. Swain[1]

Abstract

Purpose: To delineate gene expression patterns and profile changes in metastatic tumor biopsies at baseline and 1 month after treatment with the epidermal growth factor receptor (EGFR) tyrosine kinase inhibitor erlotinib in patients with metastatic breast cancer.

Experimental Design: Patients were treated with 150 mg of oral erlotinib daily. Gene expression profiles were measured with Affymetrix U133A GeneChip and immunohistochemistry was used to validate microarray findings.

Results: Estrogen receptor (ER) status by immunohistochemistry is nearly coincided with the two major expression clusters determined by expression of genes using unsupervised hierarchical clustering analysis. One of 10 patients had an EGFR-positive tumor detected by both microarray and immunohistochemistry. In this tumor, tissue inhibitor of metalloproteinases-3 and collagen type 1 α 2, which are the EGF-down-regulated growth repressors, were significantly increased by erlotinib. Gene changes in EGFR-negative tumors are those of G-protein-linked and cell surface receptor – linked signaling. Gene ontology comparison analysis pretreatment and posttreatment in EGFR-negative tumors revealed biological process categories that have more genes differentially expressed than expected by chance. Among 495 gene ontology categories, the significant differed gene ontology groups include G-protein-coupled receptor protein signaling (34 genes, $P = 0.002$) and cell surface receptor – linked signal transduction (74 genes, $P = 0.007$).

Conclusions: ER status reflects the major difference in gene expression pattern in metastatic breast cancer. Erlotinib had effects on genes of EGFR signaling pathway in the EGFR-positive tumor and on gene ontology biological process categories or genes that have function in signal transduction in EGFR-negative tumors.

Erlotinib is a selective small-molecule inhibitor of the epidermal growth factor receptor tyrosine kinase (EGFR-TK). In preclinical models, erlotinib has been shown to inhibit EGFR-TK and subsequently its downstream signaling, which lead to the growth arrest of tumor cells whose proliferation depends on EGFR signaling. Erlotinib primarily targets the EGFR-TK but at higher concentrations acts on other receptor kinases such as insulin-like growth factor I receptor (IGFIR) and insulin receptor (1, 2).

Erlotinib has been tested in various phases of clinical trials for its safety, tolerability, and treatment efficacy with the most activity seen in non – small cell lung cancer. Mutations in the EGFR-TK domain were found in non – small cell lung cancer and these mutations cause hypersensitivity to growth inhibition by gefitinib and is predictive of sensitivity to the receptor tyrosine kinase inhibitors (3, 4). In our pilot trial, 18 previously treated patients with metastatic breast cancer were given erlotinib alone at an oral dose of 150 mg daily, and no clinical responses and no significant changes in tumor proliferation after erlotinib treatment were observed (5). One tumor expressed significant levels of EGFR protein and erlotinib had inhibitory effects on the EGFR-TK of the EGFR-positive tumor as shown by the decreased activities of phosphorylated-EGFR, phosphorylated-mitogen-activated protein kinase, and phosphorylated-Akt (5). However, erlotinib had no apparent inhibitory effect on markers examined in EGFR-negative tumors. Therefore, it is of interest to further explore the effects of erlotinib in tumors that express or do not express EGFR at the gene expression profile levels.

Gene ontology is a term used to describe the genes in their associated biological processes, cellular components and molecular function (http://www.geneontology.org). Comparison analysis of gene ontology categories pretreatment and posttreatment is expected to identify the differentially expressed genes within a biological context. It is thus of interest to explore what effects erlotinib exerts on various gene ontology biological process categories in patient tumors.

Estrogen receptor (ER) has been shown to be critical in molecular classification of human primary breast cancer (6, 7). ER-positive tumors based on expression of genes were classified as epithelial/luminal-like subtype and ER-negative tumors were

Authors' Affiliations: [1]Cancer Therapeutics Branch in Center for Cancer Research and [2]Biometrics Research Branch, National Cancer Institute, NIH, Bethesda, Maryland

Received 2/7/05; revised 6/7/05; accepted 7/1/05.

The costs of publication of this article were defrayed in part by the payment of page charges. This article must therefore be hereby marked *advertisement* in accordance with 18 U.S.C. Section 1734 solely to indicate this fact.

Note: Supplementary data for this article are available at Clinical Cancer Research Online (http://clincancerres.aacrjournals.org/).

Requests for reprints: Sherry X. Yang or Sandra M. Swain, Cancer Therapeutics Branch, Center for Cancer Research, National Cancer Institute, Room 5101, Building 8, 8901 Wisconsin Avenue, Bethesda, MD 20889. Phone: 301-451-6882; Fax: 301-496-0047; E-mail: xy32m@nih.gov or swains@mail.nih.gov.

doi:10.1158/1078-0432.CCR-05-0270

defined as myoepithelial/basal-like subtype (6). However, it is largely unknown whether ER status is still associated with the gene expression pattern in metastatic breast cancer.

With 10 pairs of tumor biopsies pretreatment and posttreatment available, we have undertaken the current study in an attempt to explore the gene expression patterns in metastatic breast cancer. Furthermore, the gene expression profiles pre- and post-erlotinib in one pair of EGFR-positive and nine pairs of EGFR-negative tumor samples were compared, respectively, and the significantly changed genes were identified. Gene ontology comparison has revealed the differentially expressed gene ontology categories that have higher than expected numbers of genes between pre- and post-erlotinib in EGFR-negative tumor samples.

Materials and Methods

Patients. Patient eligibility criteria, treatment plan, and clinical and toxicity evaluation have been described previously (5). The study was approved by the Institutional Review Board of the National Cancer Institute. All patients gave written informed consent.

Tumor core biopsies and RNA extraction. Tumor core biopsies were obtained at different metastatic sites including liver, lymph node, and chest wall using an 18-gauge needle or punch biopsy (chest wall mets) at baseline and 1 month after erlotinib treatment. For each of the patients, paired biopsies were both from the same metastatic organ site. They were immediately snap-frozen and stored at −80°C until use. The presence of tumor was evaluated using H&E-stained paraffin-embedded sections and >80% of tumor cells were present in each of the core biopsies. The cores used for formalin fixation and paraffin embedding were obtained at the same time as the frozen ones. Total RNA was extracted from the tumor cores available in pairs using Trizol reagent (Invitrogen, Carlsbad, CA) recommended by Affymetrix (Santa Clara, CA; ref. 8). The RNA yields ranged from 5 to 15 μg. Quality of each RNA sample extracted from the tumor core biopsies was examined by the BioAnalyzer (Agilent Technologies, Palo Alto, CA) before the subsequent double strand cDNA, cRNA syntheses, and array hybridization.

cRNA synthesis, oligonucleotide array hybridization, and analysis. First- and second-strand cDNA were synthesized from 5 to 15 μg of total RNA using the SuperScript Double-Stranded cDNA Synthesis Kit and oligo-dT_{24}-T7 primer according to the manufacturer's instructions. cRNA synthesized was labeled with biotinylated UTP and CTP by *in vitro* transcription using T7 promoter with the double-stranded cDNA as template.

cRNA (10.0 μg) was fragmented by heat and ion-mediated hydrolysis and was hybridized to oligonucleotide arrays (HG-U133A GeneChip, Affymetrix) containing 22,215 probe sets representing 18,400 transcripts of human genes. After wash, arrays were stained with phycoerythrein-conjugated streptavidin and the fluorescence intensities were determined using a laser confocal scanner (Hewlett-Packard, Palo Alto, CA). The scanned images were analyzed using Microarray suite 5.0 (Affymetrix). Sample loading and variations in staining were standardized by scaling the average of fluorescent intensities of all genes on an array to the constant target intensity (500) for all arrays used. The signal intensity for each gene was calculated as the average intensity difference, represented by [E (PM − MM) / (number of probe pairs)], where PM and MM denote perfect match and mismatch probes. All data from ~22,215 probe sets were uploaded into the statistical package BRB-ArrayTools version 3.2 (available at http://linus.nci.nih.gov) for filtering and statistical analysis (9, 10).

Immunohistochemistry and quantitative analysis. Immunohistochemistry was used to validate the expression of EGFR, IGFBP4, and tumor proliferation (Ki67). Staining on tissue sections from formalin-fixed paraffin-embedded core biopsies was described previously (5). Antibody to IGFBP4 was purchased from Upstate Biotechnology (Lake Placid, NY) and was applied to tumor sections at a dilution of 1:500. Antibodies to EGFR (monoclonal antibody clone H11) and Ki67 (MIB-1, mouse monoclonal) were from DAKO Corp. (Carpinteria, CA). Binding of the antibodies to IGFBP4, EGFR, or Ki67 in tissue sections was amplified using Vectastain Elite avidin-biotin-peroxidase complex kits (Vector Laboratories, Burlingame, CA). Cell lines known to express EGFR (MCF10A human breast epithelial cells) and IGFBP4 (glioblastoma T98G cells) were used as the positive controls. Normal tonsil was used as the positive control for Ki67. Negative controls were done using isotype immunoglobulins appropriate to the primary antibodies used (Zymed Laboratories, South San Francisco, CA). Stained tumor core sections were scored quantitatively by an investigator (S.Y.) with the assistance of the Automated Cellular Imaging System (Chromavision, San Juan Capistrano, CA) using a previously described method (5, 11). Six areas of each tumor section were scored using a free-scoring or 40× magnification tool to generate an averaged percentage and intensity of stained tumor cells. Staining index is expressed as the percentage of staining multiplied by staining intensity after subtracting the tissue readouts of the corresponding negative control for each marker/100. Ki67 was reported as a labeling percentage.

Statistical analysis. All analyses were done on data from $\log_2$-transformed median-normalized expression values. Genes that were not present in at least 15% of the array samples were excluded from analysis with 12,325 genes retained. Among these, 20% of genes with the greatest variation among samples (1,575 genes) were used for statistical data analysis because they gave the best intrapatient reproducibility.

An average linkage unsupervised hierarchical clustering on 20 samples was done on the 1,575 median-centered genes using the correlation similarity metric (12). To identify significantly changed genes in one pair of EGFR-positive tumors, each probe set on post-therapy array (11 probes per probe set) was compared with the corresponding one of pre-therapy array using Wilcoxon's signed rank test. It was considered to be statistically significant if $P < 0.003$ for increase or $P > 0.997$ for decrease (Affymetrix Microarray Suite 5.0 Comparison Analysis). To identify significantly changed genes by erlotinib treatment in EGFR-negative tumors, data from nine pairs of EGFR-negative tumors were analyzed with a paired t test with the random variance model by BRB-ArrayTools and genes significant at the $P < 0.01$ level were reported (13).

The evaluation of which gene ontology classes are differentially expressed between pretreatment and posttreatment samples was done using a functional class scoring analysis as described by Gavlidis et al. (14). For each gene in a gene ontology class, the random variance paired t test P value for comparing pretreatment versus posttreatment samples was computed. The set of P values for a class was summarized by two summary statistics: (i) The LS summary is the average log P values for the genes in that class and (ii) the KS summary is the Kolmogorov-Smirnov statistic computed on the P values for the genes in that class. The statistical significance of the gene ontology class containing n genes represented on the array was evaluated by computing the empirical distribution of these summary statistics in random samples of n genes. Gene ontology classes with $P < 0.01$ for the LS or KS statistic are reported. Functional class scoring is a more powerful method of identifying differentially expressed gene classes than the more common overrepresentation analysis or annotation of gene lists based on individually analyzed genes. The functional class scoring analysis for gene ontology classes was done using BRB-ArrayTools.

Results

Patient and baseline clinicopathologic characteristics. Patient and clinicopathologic characteristics have been described previously (5). Briefly, these 10 patients had more than one regimen of prior chemotherapy for metastatic disease.

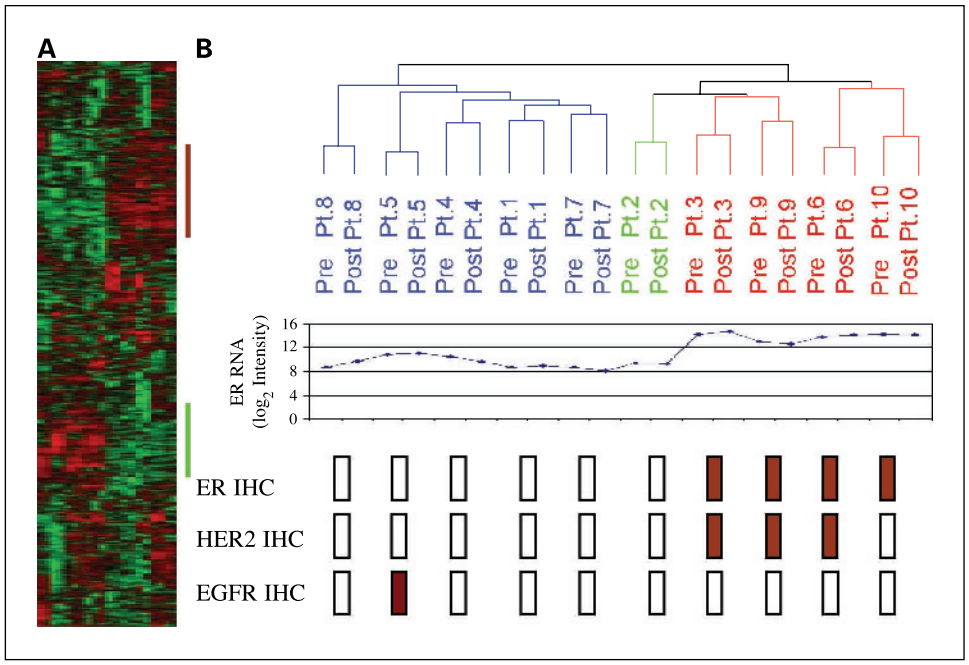

Fig. 1. *A*, hierarchical cluster analysis of 1,575 genes in 20 metastatic breast tumors. Luminal/ER gene cluster (*red bar*) and basal-like cluster (*green bar*). *B*, dendrogram showing each of tumor pairs at terminal branches (*top*). Expression of ER RNA (*middle*). Expression of ER, HER-2/*neu*, and EGFR protein by immunohistochemistry (*bottom*). ER-, HER-2/*neu*-, and EGFR-positive tumors (*red bar*) and ER-, HER-2/*neu*, and EGFR-negative tumors (*white bar*).

Five patients with ER-positive tumors and thre with HER-2/*neu*-positive tumors had received hormonal therapy or trastuzumab treatment. These metastatic tumors were from liver (three pairs), lymph nodes (three pairs), and chest wall (four pairs) and were all pathologically confirmed poorly differentiated carcinoma consistent with the breast origin.

Gene expression pattern of metastatic breast tumors pre- and post-erlotinib treatment. To investigate the intrinsic gene expression pattern in metastatic breast cancer, an average linkage hierarchical clustering approach was used to analyze the 20 tumor biopsies. As shown in the dendrogram in Fig. 1, all tumor pairs were grouped together at each of the terminal branches, suggesting the relatedness of each tumor pairs. To study the ER status in relation to the gene expression pattern, ER expression by both gene expression profiling and immunohistochemistry were aligned to tumor clusters determined by expression of genes. Most of ER-negative tumors appeared on the left major branch (*blue colored*) and ER-positive tumors on the right major branch (*red colored*) of the dendrogram. Only one ER-negative tumor pair was classified into the ER-positive cluster (*green colored*; Fig. 1B). Next, HER-2/*neu* status by immunohistochemistry was aligned to gene expression clusters. Seven tumors were HER-2/*neu* negative, in which five were in the left major expression cluster and two in the right major expression cluster of the dendrogram. Three HER-2/*neu*-positive tumors appeared in the right major expression cluster of the dendrogram (Fig. 1B). Furthermore, expression of EGFR by immunohistochemistry was aligned to the gene expression clusters. The pair of EGFR-positive tumor appeared in the left major expression cluster (Fig. 1B). Its expression at both transcriptional and protein level in 10 pairs of tumors is shown in Fig. 2, in which a high level of EGFR mRNA expression is concordant with that of EGFR protein expression in the EGFR-positive tumor.

Gene expression profile difference pre- and post-erlotinib treatment in epidermal growth factor receptor–positive and –negative tumors. As our data reported previously, EGFR-TK and its downstream signaling in the EGFR-positive tumor were decreased by erlotinib (5). To study other potential targets of erlotinib in the one EGFR-positive tumor, gene expression profiles pre- and post-erlotinib samples were compared. Examples of the decreased genes were *cyclin E2*, *cell cycle division 27*, *eukaryotic translation elongation factor 1 epsilon 1*, *MAD2-like 1*, and *c-myc* binding protein. Representatives of the increased genes were various extracellular matrix proteins such as *fibronectin 1*, *collagen, type I, α 1 and 2 (COL1A1 and 2)*, *and tissue inhibitor of metalloproteinases-1 and -3* (*TIMP-1 and TIMP-3*; Supplementary Table 1). Of note, *COL1A2* and *TIMP-3* are the EGF-down-regulated growth repressors (15). However,

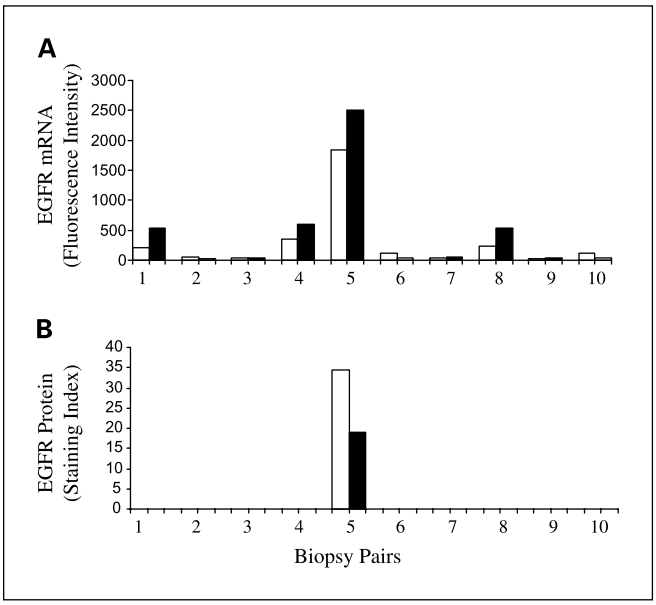

Fig. 2. Expression of EGFR mRNA (*A*) by microarray and EGFR protein (*B*) by immunohistochemistry in 10 tumor pairs pre- (*unfilled*) and post-erlotinib (*black*) treatment.

Table 1. Top 33 genes associated with erlotinib treatment in EGFR-negative tumors

Functional group by gene ontology/gene name	Gene symbol	Affymetrix probe set	Ratio of post- versus pre-therapy	*P**
G-protein signaling/coupled to cyclic nucleotide second messenger/cell surface receptor – linked signaling				
Neuropeptide Y receptor Y1	*NYP1R*	205440_s_at	0.2	0.0002
Reticulon 1	*RTN1*	203485_at	0.3	0.0021
Amyloid β (A4) precursor protein-binding, family B, member2	*APBB2*	213419_at	1.8	0.0023
Chemokine (C-C motif) receptor 1	*CCR1*	205099_s_at	0.4	0.0061
Carbamoyl-phosphate synthetase 1	*CPS1*	217564_s_at	0.4	0.0063
Defensin, β1	*DEFB1*	210397_at	0.5	0.0075
Prostaglandin E receptor 4	*PTGER4*	204897_at	0.6	0.0076
ATPase/GTPase activity/ATP binding/transporter activity				
Solute carrier family 27, membrane 2	*SLC27A2*	205768_s_at	0.4	0.0012
Alcohol dehydrogenase IB	*ADH1B*	209612_s_at	0.4	0.0045
Fatty acid – binding protein 4	*FABP4*	203980_at	0.4	0.0049
T-cell, immune regulator 1, ATPase	*TCIRG1*	204158_s_at	1.7	0.0052
Sodium bicarbonate transporter-like, membrane 10	*SLC4A10*	206830_at	2.2	0.0065
Acyl-coenzyme A oxidase 2	*ACOX2*	205364_at	0.5	0.0069
RAB31, member RAS oncogene	*RAB31*	217764_at	0.7	0.0081
ADP-ribosylation factor-like 4	*ARL4*	205020_s_at	0.5	0.0069
Drug metabolism				
Nicotinamide *N*-methyltransferase	*NNMT*	202238_s_at	0.5	0.0015
Cytochrome *P*450, family 1B1	*CYP1B1*	202437_s_at	0.6	0.0058
Cytoskeletal protein binding/extracellar matrix protein/cytoskeleton protein				
Syndecan 2	*SDC2*	212154_at	0.5	0.0048
Spondin 1	*SPON1*	213993_at	1.9	0.0056
Collagen, type VI, α 3	*COL6A3*	201438_at	0.6	0.0033
Fibronectin 1	*FN1*	212464_s_at	0.6	0.0035
Vitronectin	*VTN*	204534_at	0.3	0.0065
Collagen, type IV, α 1	*COL4A1*	211981_at	0.3	0.0083
Erythrocyte membrane protein band 4.1-like 3	*EPB41L3*	206710_at	0.4	0.0069
Keratin 6A	*KRT6A*	209126_x_at	0.6	0.0071
Keratin 17	*KRT17*	205157_s_at	0.5	0.0080
IGF binding protein 4	*IGFBP4*	201508_at	0.5	0.00220
Serine-type peptidase				
Kallikrein 10	*KLK10*	209792_s_at	0.4	0.0023
Haptoglobin-related protein	*HPR*	208470_s_at	0.3	0.0055
Nexin, plasminogen activator inhibitor type 1	*SERPINE1*	202628_s_at	0.3	0.00749
Others				
Latrophilin 3	*LPHN3*	209866_s_at	2.1	
Parvalbumin	*PVALB*	205336_at	2.9	0.0084
Caldesmon 1	*CALD1*	201617_x_at	0.4	0.0095
Tenascin C	*TNC*	201645_at	0.5	0.0097
Phospholipase A2, group IVA	*PLA2G4A*	210145_at	0.4	0.0043
Disabled homologue 2, mitogen-responsive phosphoprotein	*DAB2*	201280_s_at	0.4	0.0046
GREB 1 protein	*GREB1*	205862_at	0.3	0.0054
Par-3 partitioning defective 3 homologue	*PARD3*	210094_at	0.3	0.0055
SWAP-70 protein	*SWAP70*	209306_at	0.6	0.0083

*Paired *t* test.

these changes were not observed in tumors with low levels of EGFR in patients 1, 4, and 8 shown in Fig. 2.

To investigate the effect of erlotinib treatment on EGFR-negative tumors, the gene expression profiles pre- and post-erlotinib in nine pairs of EGFR-negative tumor were compared and the top 33 genes associated with erlotinib treatment was identified ($P < 0.01$; Table 1). Although the false discovery rate associated with the use of significance at the $P < 0.01$

level is high (16 of 33, 48%), a significant portion of the changed genes are those whose biological function is associated with the ATP or GTP molecules. These are genes encoding ATPases, GTPases, ATP or GTP binding, and various energy-dependent membrane transporters or G-protein-coupled receptor signaling pathway proteins. In addition, expression of a cytochrome *P*450 protein *CYP1B1* was decreased after erlotinib treatment.

Overall, in contrast to the EGFR-positive tumors, various EGFR-independent signaling molecules and *IGFBP4* were decreased in EGFR-negative tumors (Table 1). The decrease in *IGFBP4* expression in post- versus pre-erlotinib tumors was confirmed by immunohistochemistry at the protein level in three tumor pairs (Fig. 3A and B). In contrast, there was not much change in Ki67 at both transcriptional and protein levels (Fig. 3C and D). IGFBP4 was present in all the cellular components including tumor, inflammatory, and stroma cells before therapy but was present mainly in tumor cells with a decreased protein expression level after therapy.

Gene ontology categories differentially expressed pre- and post-erlotinib treatment in epidermal growth factor receptor–negative tumors. Because the false-discovery rate was high in our analysis at the individual gene level in EGFR-negative tumors, we did a more statistically powerful analysis based on gene ontology categories. The latter identifies genes differentially expressed pretreatment and posttreatment within biological processes. Twenty-three of 495 gene ontology categories were found differentially expressed from pretreatment to posttreatment at the $P < 0.01$ level (Table 2). Of the 16 gene ontology categories statistically significant by the LS statistic at the $P < 0.01$ level, only five false-positive categories would be expected by chance corresponding to a false discovery rate of 31% (4.95 of 16). The significantly differed gene ontology classes include G-protein-coupled receptor protein signaling pathway; serine-type endopeptidase activity, cell surface receptor–linked signal transduction, and extracellular matrix.

Discussion

Unsupervised hierarchical clustering analysis revealed that ER status by immunohistochemistry almost coincided with the two major tumor clusters defined by expression of genes in metastatic breast tumors derived from liver, lymph node, and chest wall. This indicates that in metastatic breast cancer, ER status is a key factor to determine the gene expression pattern. ER-positive metastatic breast tumor preserved the epithelial/luminal cell feature, whereas ER-negative metastatic breast tumors still have the myoepithelial/basal cell characteristics at the distinct metastatic organ sites. The pair that was "misplaced" in the dendrogram has the ER-positive gene expression pattern but lacks ER (*ESR1*) expression by both microarray and immunohistochemistry (Fig. 1B). This could be due to the inactivation of ER gene expression by the mechanism of epigenetics (8). Expression of EGFR appeared in the cluster of basal-like/ER-negative tumor, which is independent of ER expression (16).

In the EGFR-positive tumor detected by both cDNA microarray and immunohistochemistry, erlotinib treatment led to the decrease in *cyclin* E2 and *cell division cycle 27*, and the increase in *TIMP-3* and *COL1A2*. The latter two are EGF-regulated growth repressors that are the downstream targets of RAS and are specifically repressed by EGF-induced transformation (15). Therefore, these changes may have been derived from the inhibition of EGFR pathway; however, they were not translated into clinical response. The tumor likely progressed through other pathway signaling (17).

Thirty-three genes changed with erlotinib treatment were identified for the receptor-negative tumors at the $P < 0.01$ level (Table 1). Notably, *IGFBP4* was significantly decreased by erlotinib. Previously, erlotinib at higher concentrations has been shown to inhibit the kinase activity of IGFIR (1, 18). Addition of IGF-I diminished the inhibitory effect of anti-EGFR antibody on DiFi human colorectal tumor cells (18). IGF-binding proteins alter the interaction of IGFs with their cell surface receptors such as IGFIR (18). Therefore, it warrants further study to examine the effect of erlotinib on the expression of IGF-I receptor and the tyrosine kinase activities of IGF-I receptor, level of IGF-I, and IGFBPs. Gene profiling data from this cohort showed no significant change in expression of *IGF-I* mRNA and IGFIR by erlotinib (data not shown).

Overall in both EGFR-positive and EGFR-negative tumors, few apoptosis, antiapoptosis, or proliferation genes were significantly changed. This is consistent with our clinical

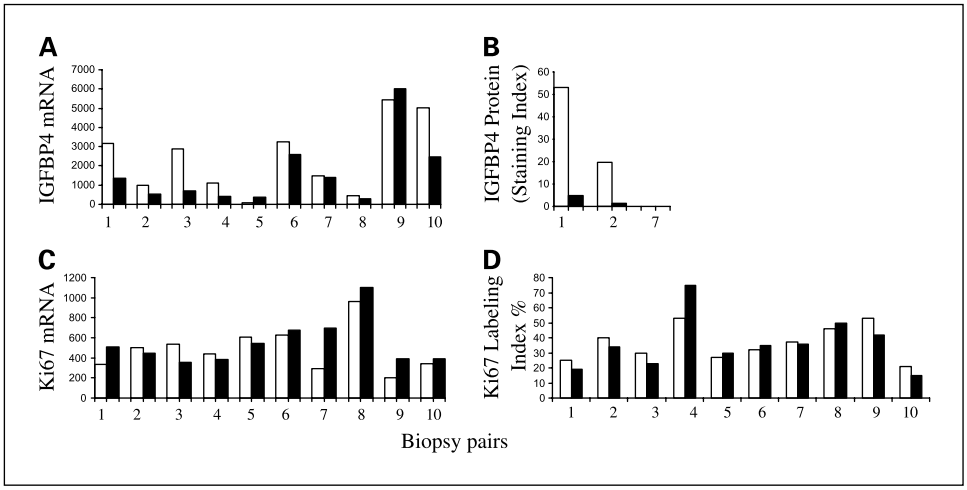

Fig. 3. Expression of IGFBP4 mRNA (*A*) and protein (*B*) and Ki67 mRNA (*C*) and protein (*D*) in 10 pairs of tumor biopsy pre- (*unfilled*) and post-erlotinib (*black*) treatment. IGFBP4 mRNA overall was called decrease shown in (*A*) in contrast to Ki67 mRNA in (*B*) for which was called no change by paired *t* tests in BRB-Array Tool. *B,* three tumor biopsy pairs that were available for analysis.

Table 2. Gene ontology category difference pre- and post-erlotinib treatment in EGFR-negative tumors

Gene ontology category	Gene ontology description	No. genes	LS permutation *P*	KS permutation *P*
0016614	Oxidoreductase activity/acting on CH-OH group of donors	13	0.00001	0.01481
0016616	Oxidoreductase activity/acting on the CH-OH group of donors/NAD or NADP as acceptor	12	0.00038	0.04089
0007178	G-protein signaling/coupled to cyclic nucleotide second messenger	6	0.00064	0.11368
0019935	Cyclic nucleotide – mediated signaling	6	0.00064	0.11368
0004263	Chymotrypsin activity	12	0.00069	0.02313
0004295	Trypsin activity	12	0.00069	0.02313
0007186	G-protein-coupled receptor protein signaling pathway	34	0.00151	0.03486
0004252	Serine-type endopeptidase activity	18	0.00153	0.01726
0042277	Peptide binding	5	0.00154	0.10926
0008236	Serine-type peptidase activity	20	0.0024	0.03944
0019932	Second messenger-mediated signaling	12	0.00466	0.17179
0007166	Cell surface receptor – linked signal transduction	74	0.00687	0.08174
0006631	Fatty acid metabolism complement activation	14	0.00699	0.09625
0006956	Complement activation	11	0.00944	0.007
0005578	Extracellular matrix (sensu Metazoa)	62	0.00944	0.00169
0031012	Extracellular matrix	62	0.00947	0.00169
0016791	Phosphoric monoester hydrolase activity	16	0.01445	0.007
0004725	Protein tyrosine phosphatase activity	6	0.0198	0.00513
0007596	Blood coagulation	15	0.02903	0.00864
0050817	Coagulation	15	0.02903	0.00864
0004721	Phosphoprotein phosphatase activity	11	0.03496	0.0059
0006470	Protein amino acid dephosphorylation	12	0.03728	0.00272
0016311	Dephosphorylation	12	0.03728	0.00272

findings (no objective responses) in this cohort of patients (5). However, the change in genes at the transcriptional level in EGFR-negative tumors are those whose function were coupled to ATP or GTP molecule including ATPases, GTPases, ATP- and GTP-binding proteins, or G-protein-coupled receptor signaling proteins (Table 1). This would not be surprising as erlotinib, the small-molecule competitive inhibitor of ATP on the EGFR-TK, may have directly or indirectly at varying levels of affinity affected other ATP- and GTP-coupling or -dependent molecules at the transcriptional level. For example, erlotinib decreased RAB31 at RNA level, a member of Ras-like small GTP-binding protein superfamily whose biological function is GTPase activity (19). Other members of the family have been found to have a role on vesicular (receptors) protein transport in both endocytic and exocytic pathways (20). It will be of interest to know if RAB31 is involved in the transport of the receptors of EGF or other growth factors. Erlotinib reduced the expression level of *CYP1B1*, which encodes a member of the cytochrome *P*450 superfamily of enzymes (21). The cytochrome *P*450 proteins are monooxygenases that catalyze many reactions involved in drug metabolism and synthesis of cholesterol, steroids, and other lipids. It has been reported that erlotinib is a substrate for CYP1B1 (22). The decrease in CYP1B1 transcription by erlotinib may be due to a feedback inhibitory mechanism, a feature commonly seen in the action of many drugs.

We used gene ontology analysis to confirm the findings at the individual gene level in EGFR-negative tumors. Gene ontology functional class analysis identified gene ontology groups differentially expressed from pretreatment to posttreatment that are generally consistent with the findings at the individual gene level. These include groups of G-protein-linked and cell surface receptor – linked signal transduction, extracellular matrix protein and protein tyrosine phosphatase activity. The other top differed gene ontology categories such as oxidoreductase activity acting on CH-OH group of donors and class of peptide binding may be due to the structural effects of erlotinib (Table 2).

In summary, we have shown in this study that ER status by immunohistochemistry is associated with the gene expression pattern determined by expression of genes in metastatic breast cancer. It seems that erlotinib had effects on the signaling pathway genes regulated by EGF in the EGFR-positive tumor besides the EGFR-TK. These data indicate that erlotinib may have hit the target but proliferation of the EGFR-positive tumor was not dependent on EGFR signaling. The significantly differed genes or gene ontology categories in pre- and post-erlotinib treatment in EGFR-negative tumors are those related to the erlotinib structural effect and molecules that have function in association with signal transduction. Gene expression profiling with larger numbers of both EGFR-positive and -negative tumors is warranted in future studies.

Acknowledgments

We thank Drs. Paul Meltzer and Stan Lipkowitz for their critical review and helpful discussion of the article and Amy Lam for her technical advice on BRB-ArrayTools.

References

1. Moyer JD, Barbacci EG, Iwata KK, et al. Induction of apoptosis and cell cycle arrest by CP-358,774, an inhibitor of epidermal growth factor receptor tyrosine kinase. Cancer Res 1997;57:4838–48.
2. Hidalgo M, Siu LL, Nemunaitis J, et al. Phase I and pharmacologic study of OSI-774, an epidermal growth factor receptor tyrosine kinase inhibitor, in patients with advanced solid malignancies. J Clin Oncol 2001; 19:3267–79.
3. Paez JG, Janne PA, Lee JC, et al. EGFR mutations in lung cancer: correlation with clinical response to gefitinib therapy. Science 2004;304:1497–500.
4. Lynch TJ, Bell DW, Sordella R, et al. Activating mutations in the epidermal growth factor receptor underlying responsiveness of non-small-cell lung cancer to gefitinib. N Engl J Med 2004;350:2129–39.
5. Tan AR, Yang X, Hewitt SM, et al. Evaluation of biologic end points and pharmacokinetics in patients with metastatic breast cancer after treatment with erlotinib, an epidermal growth factor receptor tyrosine kinase inhibitor. J Clin Oncol 2004;22:3080–90.
6. Perou CM, Sorlie T, Eisen MB, et al. Molecular portraits of human breast tumours. Nature 2000;406:747–52.
7. Gruvberger S, Ringner M, Chen Y, et al. Estrogen receptor status in breast cancer is associated with remarkably distinct gene expression patterns. Cancer Res 2001;61:5979–84.
8. Yang X, Phillips DL, Ferguson AT, et al. Synergistic activation of functional estrogen receptor (ER)-α by DNA methyltransferase and histone deacetylase inhibition in human ER-α-negative breast cancer cells. Cancer Res 2001;61:7025–9.
9. van 't Veer LJ, Dai H, van de Vijver MJ, et al. Gene expression profiling predicts clinical outcome of breast cancer. Nature 2002;415:530–6.
10. Chang JC, Wooten EC, Tsimelzon A, et al. Gene expression profiling for the prediction of therapeutic response to docetaxel in patients with breast cancer. Lancet 2003;362:362–9.
11. Tan AR, Yang X, Berman A, et al. Phase I trial of the cyclin-dependent kinase inhibitor flavopiridol in combination with docetaxel in patients with metastatic breast cancer. Clin Cancer Res 2004;10: 5038–47.
12. Eisen MB, Spellman PT, Brown PO, et al. Cluster analysis and display of genome-wide expression patterns. Proc Natl Acad Sci U S A 1998;95: 14863–8.
13. Wright GW, Simon RM. A random variance model for detection of differential gene expression in small microarray experiments. Bioinformatics 2003;19: 2448–55.
14. Pavlidis P, Qin J, Arango V, et al. Using the gene ontology for microarray data mining: a comparison of methods and application to age effects in human prefrontal cortex. Neurochem Res 2004;29:1213–22.
15. Andreu T, Beckers T, Thoenes E, et al. Gene trapping identifies inhibitors of oncogenic transformation. The tissue inhibitor of metalloproteinases-3 (TIMP3) and collagen type I α2 (COL1A2) are epidermal growth factor-regulated growth repressors. J Biol Chem 1998;273:13848–54.
16. Neskovic-Konstantinovic Z, Nikolic-Vukosavljevic D, Brankovic-Magic M, et al. Expression of epidermal growth factor receptor in breast cancer, from early stages to advanced disease. J Exp Clin Cancer Res 1999;18:347–55.
17. Camp ER, Summy J, Bauer TW, et al. Molecular mechanisms of resistance to therapies targeting the epidermal growth factor receptor. Clin Cancer Res 2005;11:397–405.
18. Wu X, Fan Z, Masui H, et al. Apoptosis induced by an anti-epidermal growth factor receptor monoclonal antibody in a human colorectal carcinoma cell line and its delay by insulin. J Clin Invest 1995; 95:1897–905.
19. Bao X, Faris AE, Jang EK, et al. Molecular cloning, bacterial expression and properties of Rab31 and Rab32. Eur J Biochem 2002;269:259–71.
20. Lanzetti L, Rybin V, Malabarba MG, et al. The Eps8 protein coordinates EGF receptor signalling through Rac and trafficking through Rab5. Nature 2000;408: 374–7.
21. Choudhary D, Jansson I, Stoilov I, et al. Metabolism of retinoids and arachidonic acid by human and mouse cytochrome p450 1b1. Drug Metab Dispos 2004;32: 840–7.
22. OSI Pharmaceuticals. Tarceva™, erlotinib hydrochloride, OSI-774. In: Investigator's brochure 2004. p. 24–8.